polymers

MDPI

Application of Melt-Blown Poly(Lactic Acid) Fibres in Self-Reinforced Composites

Dániel Vadas [1], Dávid Kmetykó [1], György Marosi [1],* and Katalin Bocz [1]

[1] Department of Organic Chemistry and Technology, Budapest University of Technology and Economics, Budafoki út 8, H-1111 Budapest, Hungary; vadas.daniel@mail.bme.hu

* Correspondence: gmarosi@mail.bme.hu; Tel.: +36-1-463-3654

Abstract: The aim of our research was to produce poly(lactic acid) (PLA) fibres with diameters in the micrometer size range, serving as the reinforcing phase in self-reinforced (SR) PLA composites. Nonwoven PLA mats were manufactured by the solvent-free melt-blowing technology. Three types of PLA differing at D-lactide content were processed with a productivity as high as 36 g/h. The crystallinity of the PLA microfibres was enhanced by thermal annealing. 2–3-fold increase in the degree of crystallinity was obtained, as measured by differential scanning calorimetry (DSC). Fibre diameters between 2-14 μm were revealed by scanning electron microscopy (SEM). Static tensile tests were performed on the nonwoven mats, showing reduced moduli of the annealed fibres due the amorphous relaxation. The PLA mats were processed via hot compaction technique and formed into SR–PLA composites. The morphological and mechanical properties of the obtained microstructural composites were comprehensively studied. Composites prepared from annealed, thermally more stable PLA nonwoven mats showed superior mechanical properties, the tensile strength improved by 47% due to the higher residual fibre content.

Keywords: poly(lactic acid); melt-blowing; nonwoven mat; self-reinforcement; thermal annealing; polymer composite

1. Introduction

As the conventional linear economic model has begun to shift towards a more sustainable circular economy – even at a moderate pace – more and more emphasis has been placed on the development of renewable and/or biodegradable polymers (collectively known as biopolymers) within the plastics industry. Compared to the rest of the plastics industry, the biopolymers market is expanding at an increasing speed [1]. Various types of natural polymers (cellulose derivatives, lignin, chitosan, pectin, alginate, polyhydroxyalkanoates, pullulan) and synthetic biopolymers (poly(glycolic acid), poly(lactic acid), poly(vinyl alcohol), polybutylene succinate, etc.) have been investigated over the last two decades [2]. Among the aimed uses we can find medical, packaging, and many industrial applications, especially in the form of biocomposites or nanobiocomposites [3-6].

The most intensively studied biopolymer, polylactic acid (PLA) has a market with a compound annual growth rate (CAGR) of 19.5%, which is expected to reach $ 5.2 billion by 2020 and $ 6,5 billion by 2025 [7,8]. The main advantage of PLA is that it can be processed using conventional methods of the plastics industry (extrusion, injection molding, thermoforming, fibre drawing, etc.) [9]. Various products can be produced using this biopolymer, inter alia, blow-molded bottles, injection-molded cups, spoons and forks [10]. Nevertheless, in order to use PLA as a raw material for durable applications, it is necessary to increase its low impact and heat resistance. Researchers have recently demonstrated that with self-reinforcement (SR), a special type of composite production, the impact resistance of PLA can be improved [11,12]. In addition, since the reinforcement and matrix material of an SR-PLA product are both composed of a PLA grade, the article remains fully biodegradable.

45 This concept fits well into a sustainable, circular economic model, so lately there has been an
46 increased scientific interest in self-reinforced biocomposites.

47   Jia et al. [13] combined oriented crystalline PLA fibres with amorphous PLA films having
48 significantly different melting points, in order to widen the processing window, which exceeded
49 30°C. With 22% fibre content (applying unidirectional orientation of the fibres) SR-PLA composites
50 with 3.29 GPa modulus and 48 MPa tensile strength were produced. Thus, the modulus increased by
51 140% and the tensile strength by 13% compared to the matrix material. It is worth mentioning that
52 with bidirectional orientation of the fibres, the modulus increased by only 74% and the tensile
53 strength decreased by 65%.

54   Somord et al. [14] produced SR-PLA composites via hot compaction of PLA fibres
55 manufactured by electrospinning. The PLA solution was prepared with a mixture of
56 dichloromethane and dimethylformamide (7:3), the fibre formation was carried out using 20 kV
57 acceleration voltage and 18 cm collector distance. Fibre mats of 0,8 g were produced within a
58 2.5-hour period, which equals a productivity of 0.32 g/hour. The crystallinity of the produced fibres
59 was 16% based on DSC measurements. After removing the fibres' moisture content with ethanol,
60 composite sheets with dimensions of 30 mm × 30 mm × 150 μm were pressed at 165°C and 6 MPa, by
61 varying the compression time from 10 to 60 seconds. The tensile strength and modulus of the
62 composites (at 20 s compaction time: σ_y = 77.5 MPa, E = 3.2 GPa) improved compared to the
63 properties of the isotropic PLA film (σ_y = 49.9 MPa, E = 2.8 GPa). Kriel et al. [15] prepared core-sheath
64 PLA fibres composed of semicrystalline core and amorphous sheat by coaxial electrospinning. The
65 bicomponent fibre structure ensured wide processing window for SR composite preparation.
66 Thermal treatment of the electrospun fibres was found to be essential to increase crystallinity and
67 mechanical strength. Nevertheless, the low productivity of electrospinning and the involved organic
68 solvents make this method hardly scalable; the application areas of electrospinning are limited to
69 small size products with high added value [16-20].

70   From feasibility point of view, the conventional fibre production techniques are more
71 advantageous, with which production can be accomplished at significantly higher speed and
72 quantities. Melt-blowing is one of the most cost-effective and versatile processes commercially
73 available to produce microfibrous products. The definition of this technique is: 'a one-step process in
74 which high-velocity air blows molten thermoplastic polymer from an extruder die tip onto a
75 conveyor to form a fine fibered web' [21]. Melt-blowing technology has also been used to
76 manufacture PLA non-woven mats targeting innovative applications such as special tissue scaffolds
77 [22] and filters [23]. However, the utilization of melt-blown PLA microfibers to form SR composites
78 has been barely studied in the literature. Recently, melt-spun core-sheat PLA fibres, providing a melt
79 processing window as wide as 40 °C, were transformed into SR-PLA composites via hot-pressing by
80 Liu et al. [24]. The hot-pressing temperature was found to have noticeable effect on the composites'
81 morphological and mechanical properties.

82   The present study demonstrates the manufacturing method of one-component microfibrous
83 PLA mats by the solvent-free melt-blowing technique, focusing on the effect of D-lactide content and
84 thermal annealing on the morphological, thermal and mechanical properties of the produced PLA
85 fibres. The obtained nonwoven mats were further processed by hot compaction to form SR-PLA
86 composites, the corresponding properties of which were investigated as well.

87

2. Materials and Methods

2.1. Materials

90   As the stereoisomeric purity of PLA significantly influences its mechanical and thermal
91 properties [25], PLA grades possessing comparable rheological properties (MFIs), but differing in
92 D-lactide content, were selected for fibre production. 3052D, 3001D and 3100HP of Ingeo™
93 Biopolymer PLA produced by NatureWorks LLC (Minnetonka, MN, USA) were chosen. Some of the
94 most relevant properties of the PLA types used are summarized in Table 1.

Table 1. Properties of the selected PLA types.

Type	3052D	3001D	3100HP
Density [g/cm^3]	1.24	1.24	1.24
MFI [g/10 perc] (210°C, 2.16 kg)	14	22	24
D-lactide content [%]	4.0	1.4	0.5
Crystalline melt temperature (T_m) [°C]	145-160	160-175*	165-180*
Glass transition temperature (T_g) [°C]	55-60	55-60*	55-60*

[1] Estimated based on DSC measurements.

2.2. Melt-blowing

PLA fibres were produced by melt-blowing from raw materials previously dried for at least 8 hours at 85°C. Quick Extruder QE TS16 02/2016A type twin-screw pharmaceutical extruder was used with an L/D ratio of 25. The four heating zones of the extruder were heated to 200°C, the die temperature was 170°C and the screw speed was set to 15 rpm. A specially designed adapter was attached to the extruder die to allow the formation of sufficiently fine fibres and an appropriate flow of hot air, i.e. the melt-blowing process. The die had 330 μm diameter holes next to each other and the compressed air with an overpressure of 1 bar was heated by an AHP-7562 type device supplied by OMEGA Engineering INC. The air temperature was set to 300°C. For the collection of PLA microfibres, a hemispherical sieve made of metal mesh placed at 25 cm distance from the die was used. By means of melt-blowing, 0.6 to 0.7 g of fabric was produced per minute, corresponding to a productivity of 36 g/h. This is 110-130 times higher than the productivity of the electrospinning method used by Somord et al. [14].

2.3. Thermal Annealing

The produced melt-blown webs are largely amorphous due to rapid cooling, and since the crystalline fraction plays a key role in the production of composites, thermal annealing experiments were carried out above glass transition temperature (T_g). Samples of the microfibrous mats were placed into an 85°C oven for 2 hours. In the first hour, samples were taken every 15 minutes and then after 120 minutes on which the effect of post-crystallization was investigated by DSC.

2.4. Composite Preparation

SR-PLA composites were prepared from annealed and non-annealed nonwoven PLA mats of the 3100HP type PLA, which proved to be the most promising material. In the case of non-annealed mats, the moisture was removed by drying for 1 hour at 50°C to avoid hydrolysis during hot compaction. From the webs 26,6 × 26,6 mm squares were cut, which were layered into a square mould with 30 × 30 × 0.4 mm dimensions. The mould was placed between two metal sheets coated with polytetrafluoroethylene (PTFE) foils. The hot compression process was carried out with a Collin GmbH Teach-Line Platen Press 200E hydraulic press at 165°C and 60 bars for 4 different durations (10, 20, 30 and 60 seconds) in the case of annealed mats. Non-annealed fibres were also processed at 160°C, 60 bars, for 20 seconds, using the same apparatus. After the hot compression was completed, the mould was cooled to room temperature via cooling water in 7 minutes under pressure.

2.5. Scanning Electron Microscopy (SEM)

JEOL JSM-6380LA type scanning electron microscope (Tokyo, Japan) was used to examine the morphology of the fibres and the microstructure of the composites. The SEM images were taken with an accelerating voltage of 15 keV. All the samples were coated with gold–palladium alloy before examination in order to prevent charge build-up on the surface.

2.6. Differential Scanning Calorimetry

134 The thermal properties of the fibres were studied using a TA Instruments Q2000 type
135 calorimeter (New Castle, DE, USA). DSC measurements were carried out at a heating rate of 10°C
136 /min under 50 ml/min nitrogen gas flow, covering a temperature range of 30–200°C. About 4–9 mg
137 of sample was measured in each test, using 26,4 mg aluminum pans. The degree of crystallinity (χ)
138 of the samples was calculated according to Equation (1):

$$X = \frac{\Delta H_m - \Delta H_{cc}}{\Delta H_f} * 100 \quad [\%], \tag{1}$$

139 where ΔH_m indicates the melting enthalpy, ΔH_{cc} is the cold crystallization enthalpy, ΔH_f is the
140 melting enthalpy of the 100% crystalline PLA equal to 93 J/g [26].

141 *2.7. Tensile testing*

142 Static tensile tests were performed on the annealed and non-annealed microfibrous mats, and
143 also on the SR composites. Samples (7.5 mm × 30 mm) of the microfibrous mats and specimens
144 (3 mm × 30 mm) of the SR composites were cut out and tested on a ZWICK Z005 universal testing
145 machine (Zwick GmbH & Co. KG, Ulm, Germany). For the samples of the mats, a 20 N load cell was
146 used, the initial grip separation was 11 mm, and the crosshead speed was set to 5 mm/min.
147 Regarding the composite specimens, the measurements were performed on a 5 kN load cell, with an
148 initial grip separation of 10 mm, and crosshead speed of 1 mm/min.

149 **3. Results and Discussion**

150 *3.1. Fibre morphology*

151 The morphology of the nonwoven mats and the fibre diameters were investigated by SEM
152 analysis. As it can be observed in the images with magnifications of ×100 and ×1000 (Figure 1), PLA
153 fibres are randomly stacked in several layers, showing longitudinal bonding in numerous locations.
154 The average fibre diameters and the fibre diameter distributions of the prepared three types of PLA
155 nonwoven mats are shown in Figure 2 and Figure 3, respectively. The diameter of the melt-blown
156 fibres varies between 2 and 14 μm for each type of PLA used, which is greater than the diameter of
157 fibres produced by electrospinning in the literature [14]. In Figure 2, a decreasing tendency of fibre
158 diameters may be observed as a function of PLA's D-lactide content, but the difference is not
159 significant. The measured fibre diameter values (at least 70 fibres were measured from each type of
160 PLA nonwoven mat) have been statistically tested, and we could reject the null hypothesis that the
161 slope of the regression line for the fibre diameters of increasing D-lactide contents is zero (H_0: $\beta_1 = 0$),
162 but with a probability value of p = 0.045 which is close to the generally used significance level of α
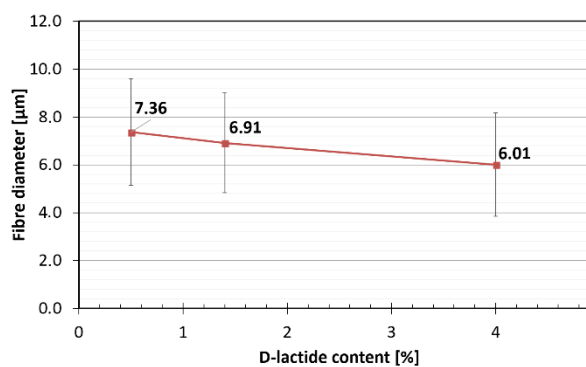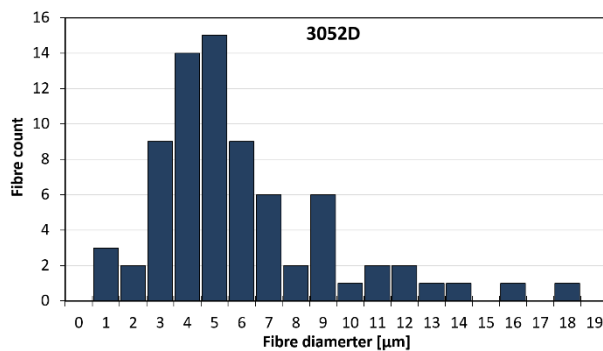163 =0.05.
164

(a)　　　　　　　　　　(b)　　　　　　　　　　(c)

165

(**d**)   (**e**)   (**f**)
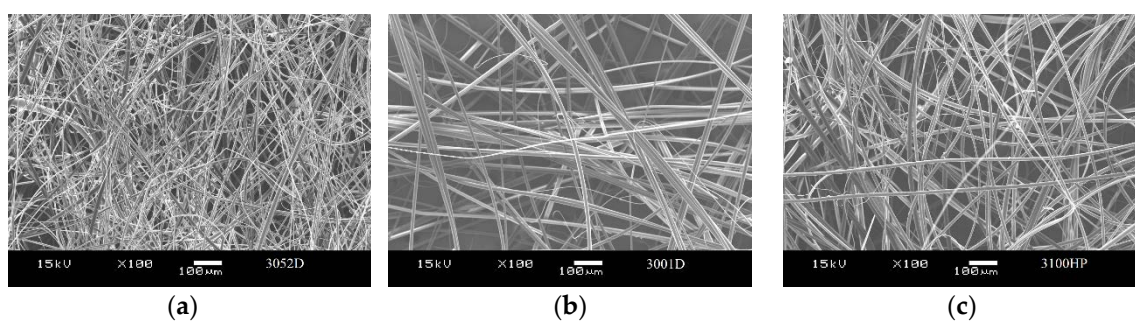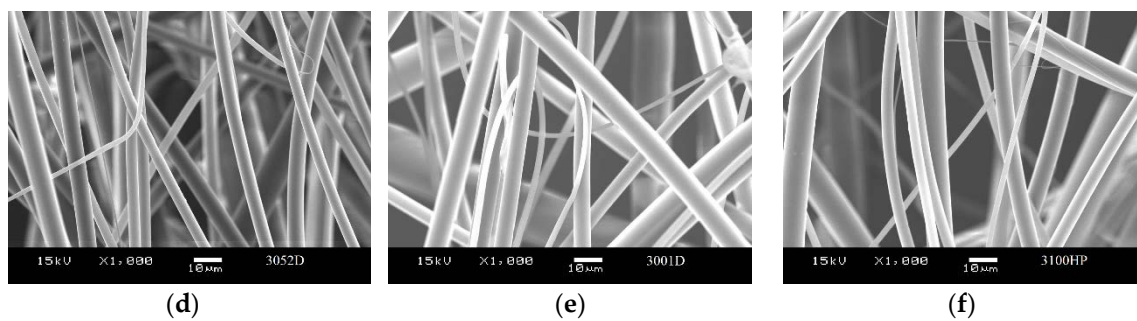
Figure 1. SEM images of the melt-blown PLA nonwoven mats: (**a,d**) 3052D; (**b,e**) 3001D; (**c,f**) 3100 HP. Magnification: ×100, ×1000

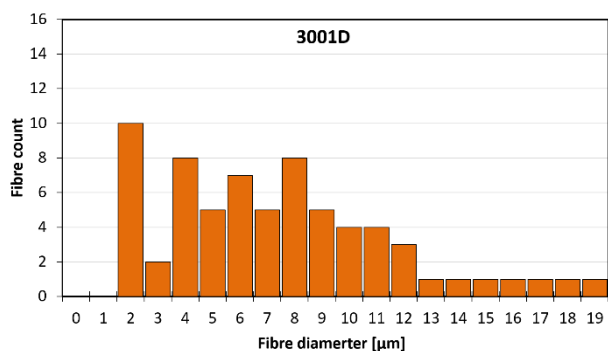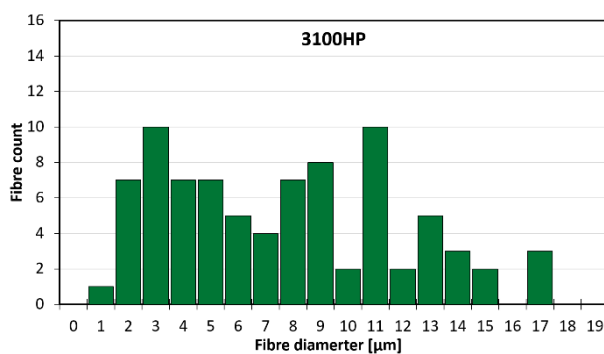**Figure 2.** Diameters of the melt-blown PLA fibres

(**a**)

(**b**)

(**c**)

Figure 3. Diameter distribution of fibres obtained from 3052D (**a**), 3001D (**b**) and 3100HP (**c**) grade PLA

3.2. Thermal properties, crystallinity

DSC analyses were carried out to investigate the thermal properties and crystallinity of the annealed and non-treated fibres. As it can be seen in Figure 4, depending on the D-lactide content of the used PLA type, 2 to 7-fold increase in crystallinity was reached after two hours of annealing. Nevertheless, it can be observed that this procedure erases the thermal history of the polymer and creates a new structure. During melt-blowing process, orientation and alignment of the PLA macromolecules in the direction of the fiber axis occurred, initiating crystallization and ordering of the amorphous region at the same time. Annealing at 85°C, above the glass transition temperature of PLA (~60-66°C), enhances segmental mobility and the oriented polymer chains are trying to return to their thermodynamically more stable form. These phenomena explain the decrease in crystallinity in the first period (15 min) of thermal annealing. For the 3100HP type PLA, the two processes compensate each other, so that total crystallinity is not reduced. Then, during cold crystallization, the amorphous parts of the macromolecules are reorganized, but the longitudinal axis of the fibre is not a preferred direction anymore, and the crystallinity shows increasing tendency as a function of annealing time for all polymer types.
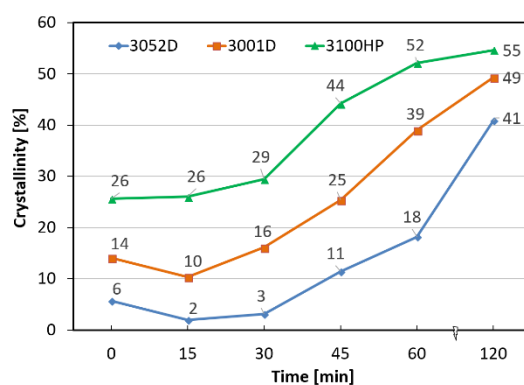
**Figure 4.** Crystallinity of PLA fibres as a function of annealing time

The thermal transitions of the PLA fibres with differing D-lactide-contents can also be observed on the corresponding DSC curves (Figures 5). In the case of non-annealed (0 min) samples, the T_g is observed around 66°C. On the curves of the annealed fibres, this phenomenon is marked by a much smaller thermal effect as the frozen-in strains induced during the melt-blowing process are eliminated in 15 minutes. As the crystallinity increases with the annealing time, the exothermic peak of cold crystallization decreases, after 30 minutes of annealing it is barely noticeable. Regarding the samples annealed for 2 hours, this heat transition is not visible at all, indicating that the fibres have reached their maximum crystallinity.

It can be noticed that after 15 minutes of thermal treatment, the cold crystallization peak temperature is significantly increased. The shift of cold crystallization exotherm to lower temperature of the non-treated fibres is attributed to the strain-induced nucleation enhanced crystallization of the stretched amorphous phase. As there is no orientation in the annealed fibres, the ordering of the macromolecules requires extra energy (higher temperature). At higher D-lactide content (Figure 5 **a**), this effect causes a significant difference, but it is barely noticeable for 3100HP (Figure 5 **c**), as in the latter case the crystallization is facilitated by the presence of the high amount of pre-existing crystals ($\chi = 26\%$). By increasing the heat treatment time, the cold crystallization peak temperatures show a slightly decreasing tendency in all cases, which is also due to the increasing crystallinity.
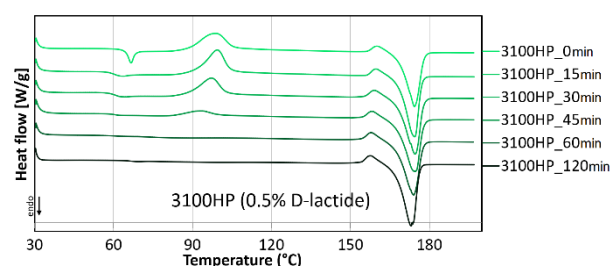
(**a**)

(**b**)

(**c**)
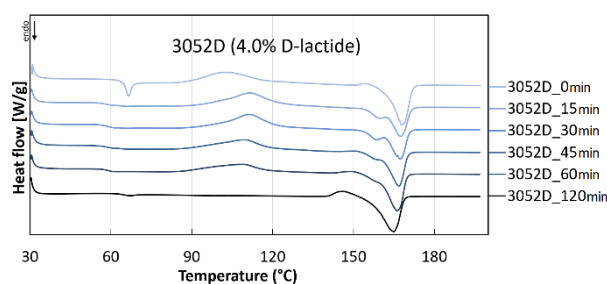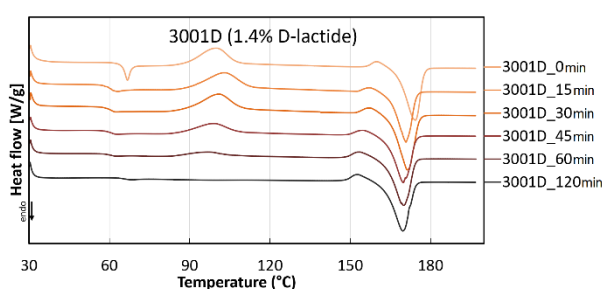
Figure 5. Thermograms of 3052D (a), 3001D (b) and 3100HP (c) type PLA annealed for 0–120 minutes

For the annealed 3052D (15–60 minutes) PLA fibres (Figure 5 **a**), double endothermic crystalline melting peak can be observed, which means that both crystalline forms of PLA (the less ordered α' and the more ordered α crystalline forms) are present. The smaller peak at 159°C shows the melting of the α' form and the recrystallization of the α crystal form, the larger peak refers to the melting of the α form. The 3052D type PLA contains the highest amount of D-lactide (4.0%), which decreases regularity of the macromolecules, so that α' crystalline form can occur. It can be seen that after 120 minutes, these less ordered crystalline structures are also transformed into a thermally more stable α crystalline form. This curve as well as the ones of 3001D and 3100HP PLA types show a smaller exothermic peak prior to crystalline melting. From this we can conclude that during the heat treatment α' is formed and this exothermic peak indicates the solid phase transformation into the

226 more stable α form, occurring in the DSC apparatus [27]. The crystalline melting peak temperature
227 increases with decreasing D-lactide content (3052D: 167°C, 3001D: 172°C, 3100HP: 175°C), this effect
228 is also due to the higher macromolecular regularity of the optically pure PLA types.
229

230 *3.3. Mechanical properties of the microfibrous mats*

231 The results of the tensile tests are shown in Figure 6. The mechanical characteristics of the
232 melt-blown microfibrous mats are comparable with the modulus and strength of electrospun PLA
233 nonwoven mats, as found in the literature [28]. It can be noticed that the Young's moduli of the
234 annealed mats are much smaller than that of the non-annealed mats obtained from the same
235 material. This phenomenon can be explained by macromolecular processes occuring during heat
236 treatment; during thermal treatment the amorphous orientation formed in the PLA fibres is relaxed,
237 so the modulus is also reduced [29]. Regarding tensile strength – except for the 3100HP type – the
238 non-annealed mats also outperform the annealed ones. As the tensile strength is more influenced by
239 the orientation of the crystalline part, the differences between the values are smaller.
240

(**a**)   (**b**)
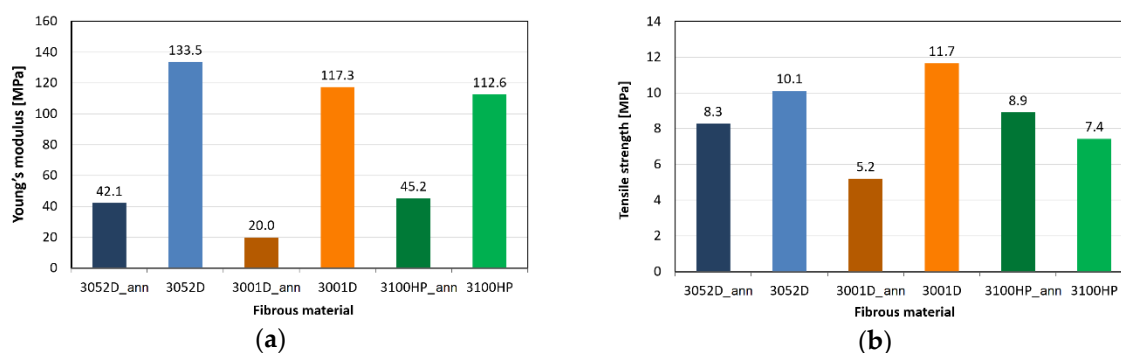
241 **Figure 6.** Young's modulus (**a**) and tensile strength (**b**) of annealed (ann) and non-annealed PLA
242 mats

243 *3.4 Mechanical properties of SR composites*

244 Based on the DSC measurements, crystallinity data and mechanical properties of the
245 melt-blown PLA nonwoven mats, 3100HP type PLA was selected for SR composite preparation. The
246 typical stress-strain curves of the obtained composites can be seen in Figure 7, while modulus and
247 tensile strength values are shown in Figure 8.
248
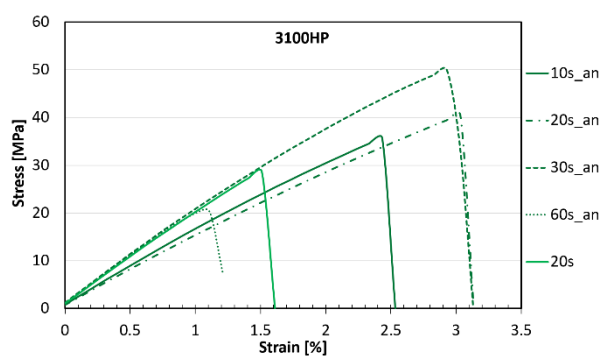
249 **Figure 7.** Stress-strain curves of SR-PLA composites
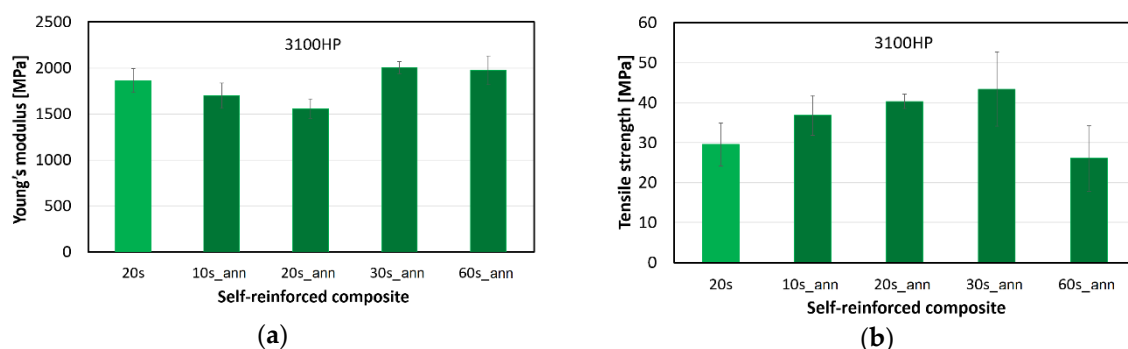
Figure 8. Young's modulus (**a**) and tensile strength (**b**) of SR composites made of annealed (ann) and non-annealed PLA mats, indicating hot compaction time (10–60 sec)

In contrast to the tensile test results of the nonwoven mats, annealed fibres compacted for 30 seconds (30s_ann) show slight improvement in modulus when compared to SR-PLA specimens composed of non-treated mats (20s). The significant effect of thermal treatment of the fibrous mats was also evinced by the obtained 47% increase in tensile strength, reaching 43 ± 9 MPa in the case of the 30s_ann composite. The favorable mechanical properties are in connection with the high crystallinity achievable in the case of the low (0.5%) D-lactide containing PLA type, providing suitable thermal resistance for processing by hot compaction. However, 60 seconds of hot compression resulted in noticeable deterioration of elongation at break (Figure 7) and tensile strength (Figure 8 **a**) values of the SR-PLA composite, likely due to the partial melting and fusion of the microfibers and also to their physical ageing occurring during the longer processing time.

3.5. Morphology of the SR-PLA composites

The fracture surfaces of the SR-PLA specimens were analyzed by SEM. Based on the SEM micrographs presented in Figure 9, conclusions regarding the consistency, fibre orientation and failure mechanism of the composites can be drawn. Despite the 5°C lower processing temperature but identical hot compaction time (20 s), significantly lower amount of reinforcing fibre can be noticed in the fracture surface of the composite made from non-treated PLA mats (Figure 9 **a)**, while fibres that have undergone thermal annealing mostly remained intact during processing (Figure 9 **b**). The more than 2-fold increase in crystallinity resulted in higher thermal resistance of the microfibres, thus lower sensitivity to the high compression temperature.
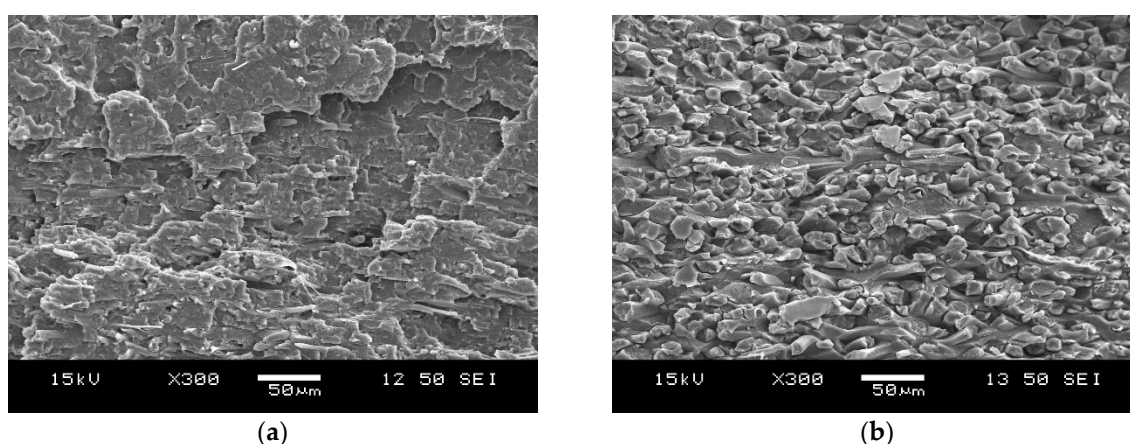
Figure 9. SEM images of SR-PLA composites made of non-annealed (**a**) and annealed (**b**) fibres with 0.5% D-lactide content (3100HP) Magnification: ×300

In the SEM images three different failure modes can be observed, namely fibre pullout, fibre/matrix debonding and brittle failure of fibres. Composites made from highly amorphous fibres

broke with plastic deformation, but specimens with higher crystallinity suffered brittle fibre failure. In the case of the SR composite composed of thermally annealed microfibers, only a suitable fraction (surface) of the reinforcing fibres have molten during processing, forming the matrix phase, and thus well-consolidated composites could be obtained. In this case self-reinforcement was successfully implemented.

5. Conclusions

In this work, PLA microfibrous nonwoven mats, serving as precursors for self-reinforced composite preparation, were prepared by melt-blowing technology. Fibres with diameters ranging between 2-14 μm were obtained with a productivity of 36 g/h from three types of PLA grades differing at D-lactide contents. The crystalline fractions of the obtained fibres were significantly increased by thermal annealing at 85°C for 2 hours with the aim to improve their thermal resistance. The heat treatment induced, however, relaxation of the molecular orientation in the fibres, and thus decreased moduli was measured for the annealed fibres. Nevertheless, self-reinforced composites with improved mechanical performance and adequate morphology could only be obtained from thermally pre-treated fibres. The improved thermal resistance of the highly crystalline PLA microfibres proved to be of key importance regarding the ability of partial melting i.e. matrix formation and to obtain adequate consolidation quality by hot compaction.

Conflicts of Interest: The authors declare no conflict of interest.

References

1. European Bioplastics: Facts and figures. Available online: http://docs.european-bioplastics.org/publications/EUBP_Facts_and_figures.pdf (accessed on 11.06.2018)

2. Haniffa, M.A.C.M.; Ching, Y.C.; Abdullah, L.C.; Poh, S.C.; Chuah, C.H. Review of bionanocomposite coating films and their applications. *Polymers* **2016**, *8(7)*, 246. https://doi.org/10.3390/polym8070246

3. Souza, V.G.L.; Pires, J.R.A.; Vieira, É.T.; Coelhoso, I.M.; Duarte, M.P.; Fernando, A.L. Shelf life assessment of fresh poultry meat packaged in novel bionanocomposite of chitosan/montmorillonite incorporated with ginger essential oil. *Coatings* **2018**, *8(5)*, 177. https://doi.org/10.3390/coatings8050177

4. Mistretta, M.C.; Botta, L.; Morreale, M.; Rifici, S.; Ceraulo, M.; Mantia, F.P.L. Injection molding and mechanical properties of bio-based polymer nanocomposites. *Materials* **2018**, *11(4)*, 613. https://doi.org/10.3390/ma11040613

5. Bertolino, V.; Cavallaro, G.; Lazzara, G.; Merli, M.; Milioto, S.; Parisi, F.; Sciascia, L. Effect of the biopolymer charge and the nanoclay morphology on nanocomposite materials. *Ind. Eng. Chem. Res.* **2016**, *55(27)*, 7373-7380. https://doi.org/10.1021/acs.iecr.6b01816

321   6.   Bertolino, V.; Cavallaro, G.; Lazzara, G.; Milioto, S.; Parisi, F. Halloysite nanotubes sandwiched between
322   chitosan layers: a novel bionanocomposite with multilayer structure. *New J. Chem.*, **2018**, *42*, 8384-8390.
323   https://doi.org/10.1039/C8NJ01161C

324   7.   Allied Market Research: Polylactic Acid (PLA) Market - Global Opportunity Analysis and Industry
325   Forecast, 2012 – 2020. Available online: https://www.alliedmarketresearch.com/polylactic-acid-market
326   (accessed on 11.06.2018)

327   8.   Grand View Research: Lactic Acid Market Size Worth $9.8Bn By 2025 & PLA To Reach $6.5Bn. Available
328   online: https://www.grandviewresearch.com/press-release/global-lactic-acid-and-poly-lactic-acid-market
329   (accessed on 11.06.2018)

330   9.   Södergard, A.; Stolt, M. Properties of lactic acid based polymers and their correlation with composition.
331   *Prog. Polym. Sci.* **2002**, *27*, 1123-1163. http://doi.org/10.1016/S0079-6700(02)00012-6

332   10.   Ajioka, I.; Enomoto, K.; Suzuki, K.; Yamaguchi, A. The basic properties of poly(lactic acid) produced by
333   the direct condensation polymerization of lactic acid. *J. Environ. Polym. Degr.* **1995**, *3(4)*, 225-234.
334   https://doi.org/10.1007/BF02068677

335   11.   Bocz, K.; Domonkos, M.; Igricz, T.; Kmetty, Á.; Bárány, T.; Marosi, G. Flame retarded self-reinforced
336   poly(lactic acid) composites of outstanding impact resistance. *Composites Part A* **2015**, *70*, 27-34.
337   https://doi.org/10.1016/j.compositesa.2014.12.005

338   12.   Mai, F.; Tu, W.; Bilotti, E.; Peijs, T. Preparation and properties of self-reinforced poly(lactic acid)
339   composites based on oriented tapes. *Composites Part A* **2015**, *76*, 145-153.
340   https://doi.org/10.1016/j.compositesa.2015.05.030

341   13.   Jia, W.; Gong, R. H.; Hogg, P. J. Poly (lactic acid) fibre reinforced biodegradable composites. *Composites*
342   *Part B* **2014**, *62*, 104-112. https://doi.org/10.1016/j.compositesb.2014.02.024

343   14.   Somord, K.; Suwantong, O.; Tawichai, N.; Peijs, T.; Soykeabkaew, N. Self-reinforced poly(lactic acid)
344   nanocomposites of high toughness. *Polymer* **2016**, *103*, 347–352.
345   https://doi.org/10.1016/j.polymer.2016.09.080

346   15.   Kriel, H.;Sanderson, R.D.; Smit, E. Single polymer composite yarns and films prepared from heat bondable
347   poly(lactic acid) core-shell fibres with submicron fibre diameters. *Fibres. Text. East Eur.* **2013**. *21, 4(100)*,
348   44-47. https://doi.org/10.5604/12303666.1196607

349   16.   Bognitzki, M.; Czado, W.; Frese, T.; Schaper, A.; Hellwig, M.; Steinhart, M.; Greiner, A.; Wendorff, J.H.
350   Nanostructured Fibers via Electrospinning. *Adv. Mater.* **2001**, *13(1)*, 70-72.
351   https://doi.org/10.1002/1521-4095(200101)13:1<70::AID-ADMA70>3.0.CO;2-H

352   17.   Dicastillo, C. L.; Roa, K.; Garrido, L.; Pereira, A.; Galotto, M.J. Novel Polyvinyl Alcohol/Starch Electrospun
353   Fibers as a Strategy to Disperse Cellulose Nanocrystals into Poly(lactic acid). *Polymers* **2017**, *9(4)*, 117.
354   https://doi.org/10.3390/polym9040117

355   18.   Farkas, B.; Balogh, A.; Farkas, A.; Domokos, A.; Borbás, E.; Marosi, G.; Nagy, Z.K. Medicated Straws Based
356   on Electrospun Solid Dispersions. *Periodica Polytechn., Chem. Eng.* **2018**, *62(3)*, 310-316.
357   https://doi.org/10.3311/PPch.11931

358   19.   Liu, Y.; Liang, X.; Wang, S.; Qin, W.; Zhang, Q. Electrospun Antimicrobial Polylactic Acid/Tea Polyphenol
359   Nanofibers for Food-Packaging Applications. *Polymers* **2018**, *10(5)*, 561.
360   https://doi.org/10.3390/polym10050561

361   20.   Borbás, E.; Sinkó, B.; Tsinman, O.; Tsinman, K.; Kiserdei, É.; Démuth, B.; Balogh, A.; Bodák, B., Domokos,
362   A.; Dargó, G.; Balogh, G.T.; Nagy, Z.K. Investigation and mathematical description of the real driving
363   force of passive transport of drug molecules from supersaturated solutions. *Mol. Pharmaceutics*, **2016**,
364   *13(11)*, 3816–3826. https://doi.org/10.1021/acs.molpharmaceut.6b00613

365   21.   Wehmann, M.; McCulloch, W.J.G. Melt blowing technology. In *Polypropylene. An A-Z reference*,
366   Krager-Kocsis, J., Eds.; Springer: Dordrecht, Netherlands, 1999; Volume 2, pp. 415-420, ISBN
367   978-94-011-4421-6 https://doi.org/10.1007/978-94-011-4421-6_58

368   22.   Hammonds, R.L.; Gazzola, W.H.; Benson, R.S. Physical and thermal characterization of polylactic acid
369   meltblown nonwovens. *J. Appl. Polym. Sci.* **2014**, *131*, 40593. https://doi.org/10.1002/app.40593

370   23.   Liu, Y.; Cheng, B.; Cheng, G. Development and filtration performance of polylactic acid meltblowns. *Text.*
371   *Res. J.* **2010**, *80(9)*, 771–779 https://doi.org/10.1177/0040517509348332

372   24.   Liu, Q.; Zhao, M.; Zhou, Y.; Yang, Q.; Shen, Y.; Gong, R.H.; Zhou, F.; Li, Y.; Bingyao, Deng. Polylactide
373   single-polymer composites with a wide melt-processing window based on core-sheath PLA fibers. *Mater.*
374   *Design.* **2018**, *139*, 36-44. https://doi.org/10.1016/j.matdes.2017.10.066

25. Puchalski, M.; Kwolek, S.; Szparaga, G.; Chrzanowski, M.; Krucinska, I. Investigation of the Influence of PLA Molecular Structure on the Crystalline Forms (α' and α) and Mechanical Properties of Wet Spinning Fibres. *Polymers* **2017**, *9(1)*, 18. https://doi.org/10.3390/polym9010018

26. Fischer, E.W.; Sterzel, H.J.; Wegner, G. Investigation of the structure of solution grown crystals of lactide copolymers by means of chemical reactions. *Colloid. Polym. Sci.* **1973**, *251*, 980–990. http://doi.org/10.1007/BF01498927

27. Tábi, T.; Hajba, S.; Kovács, J.G. Effect of crystalline forms (α' and α) of poly(lactic acid) on its mechanical, thermo-mechanical, heat deflection temperature and creep properties. *Eur. Polym. J.* **2016**, *82*, 232–243. http://doi.org/10.1016/j.eurpolymj.2016.07.024

28. Gualandi, C.; Govoni, M.; Foroni, L.; Valente, S.; Bianchi, M.; Giordano, E.; Pasquinelli, G.; Biscarini, F.; Focarete, M. L. Ethanol disinfection affects physical properties and cell response of electrospun poly(L-lactic acid) scaffolds. *Eur. Polym. J.* **2012**, *48*, 2008-2018. https://doi.org/10.1016/j.eurpolymj.2012.09.016

29. Flood, J.E.; Nulf, S.A. How molecular weight distribution and drawing temperature affect polypropylene physical properties and morphology. *Polym. Eng. Sci.* **1990**, *30*, 1504–1512. https://doi.org/10.1002/pen.760302304